EFFICIENT MULTIDIMENSIONAL PARAMETER ESTIMATION FOR JOINT WIDEBAND RADAR AND COMMUNICATION SYSTEMS BASED ON OFDM

Jianshu Zhang[1]*, Ivan Podkurkov*[2]*, Martin Haardt*[1]*, and Adel Nadeev*[2]

[1]Communications Research Laboratory, Ilmenau University of Technology, Germany, [2]German-Russian Institute of Advanced Technologies, Tupolev Kazan National Research Technical University, Russia

ABSTRACT

In this paper we study the parameter estimation problem of an OFDM based joint wideband SIMO radar and communication system. The parameters to be estimated are time delays, relative velocities, and angle of arrival (DoA) pairs of radar targets. Due to the wideband assumption the received signal on different subcarriers are incoherent and therefore cannot fully exploit the frequency diversity of the OFDM waveform. In order to estimate the parameters jointly and coherently on different subcarriers, we propose an interpolation based coherent multidimensional parameter estimation framework, where firstly the wideband system model is transformed into an equivalent narrowband system model, and then multidimensional parameter estimation algorithms can be applied. More precisely, a wideband R-D periodogram is introduced as a benchmark algorithm and a high-resolution R-D Wideband Unitary Tensor-ESPRIT algorithm is proposed. Simulation results show that the proposed coherent parameter estimation method significantly outperforms the direct application of multidimensional parameter estimation algorithms to the wideband model.

Index Terms— Joint radar and communication, wideband OFDM, Periodogram, Interpolation, ESPRIT.

I. INTRODUCTION

A joint radar and communication system, namely the communication radar, can exploit the available physical resources such as spectrum and hardware components more efficiently compared to a traditional radar or communication system [1], [2]. To facilitate the equalization in a frequency selective environment, typically OFDM waveforms are used [3], [4]. The performance of such a joint radar-communication system was analysed in [5], [6]. Since a communication radar is promising for applications such as intelligent transportation systems (ITSs) [7], [8], it has been recently studied in [2] and [9]. In [2] the OFDM communication radar is build based on the sub-6 GHz car-to-car communication standard, i.e., IEEE 802.11p. The estimation of target distances and velocities has been studied and a one-dimensional periodogram based algorithm has been proposed and analyzed. In [9] the communication radar is built based on the mmWave WLAN standard, i.e., IEEE 802.11ad. A time domain correlation based parameter estimation method has been proposed. In both papers a narrowband system is considered and the proposed parameter estimation methods are search-based non-parametric methods. However, for critical scenes subspace-based high-resolution algorithms are preferred because they can provide more accurate estimates. Moreover, since the distance resolution of a radar is proportional to the bandwidth, the future communication radar is likely to have a large bandwidth.

Therefore, this motivates us to study a joint wideband radar and communication system. In this paper we focus on the radar estimation problem under a wideband assumption. More precisely, we develop parameter estimation methods for a communication radar based on OFDM waveforms and, without loss of generality, use a uniform rectangular array (URA) at the receiver. Unlike a narrowband system, the wideband assumption results in different phase shifts on different subcarriers and therefore different spatial frequencies on each subcarrier [10]. These frequency imperfections will cause a significant performance degradation if they are not dealt with. Therefore, we propose an interpolation based coherence parameter estimation framework to estimate time delays, relative velocities, and angle of arrival (DoA) pairs of radar targets. To this end, the wideband system model is transformed into an approximately equivalent narrowband system by using interpolation methods. This is only approximate since practically interpolation errors cannot be avoided. After that, the parameters are estimated by using the proposed multidimensional parameter estimation methods on the equivalent narrowband system model. To this end, a low resolution R-D periodogram is developed and used as a baseline algorithm. The high resolution R-D Unitary Tensor-ESPRIT in [11] is also extended to our scenario. Simulation results show that the proposed multidimensional parameter estimation methods provide a significant performance gain over the direct application of multidimensional parameter estimation methods in such a wideband system. In [10], the authors also use an interpolation technique for the same problem, but only the Shannon-Whittaker interpolation method is applied to a one-dimensional problem, followed by a 3-D canonical polyadic (CP) decomposition based parameter estimation method, which can also be extended to our problem. However, the CP decomposition has a significantly higher computational complexity compared to the HOSVD, which will be used in our application. Moreover, we decompose a real-valued tensor that has the same dimensionality as its complex-valued counterpart, which reduces the computational complexity even further.

Notation: Upper-case and lower-case bold-faced letters denote matrices and vectors, respectively. The expectation, conjugate, Hermitian transpose, and Moore-Penrose pseudo inverse are denoted by $\mathbb{E}\{\cdot\}$, $\{\cdot\}^*$, $\{\cdot\}^{\mathrm{H}}$, and $\{\cdot\}^+$, respectively. The $m \times m$ identity matrix is $\boldsymbol{I}_m$. Moreover, the $m \times m$ exchange matrix with ones on its antidiagonal and zeros elsewhere is $\boldsymbol{\Pi}_m$. The $m \times m$ left-$\boldsymbol{\Pi}$-real matrix $\boldsymbol{Q}_m$ satisfies $\boldsymbol{\Pi}_m \boldsymbol{Q}_m^* = \boldsymbol{Q}_m$. Furthermore, the absolute value is denoted by $|\cdot|$, the concatenation of matrices or tensors along the r-th dimension is denoted by $\sqcup_r$ ($r = 1, 2, 3, 4$) [11], and the outer product between multi-linear vectors is $\circ$ [11]. The r-mode product between a tensor and a matrix is $\times_r$ [12].

II. SYSTEM MODEL

We consider an OFDM based communication radar with a co-located single transmit antenna and multiple receive antennas. The receive antenna array is a $M_{\mathrm{x}} \times M_{\mathrm{y}}$ uniform rectangular array. We assume that the radar and the communication system have different baseband units but use the same RF components [2]. To avoid a full-duplex operation of the communication system, the radar and the communication system can transmit simultaneously but will not receive simultaneously on the same subcarrier at the same time. Since the two systems can work independently, in this paper we focus on the radar function, i.e., the detection of targets. The h-th

radar target ($h \in \{0, \cdots, H-1\}$) is parametrized by the time delay $\tau_h = \frac{2d_h}{c}$, where d_h denotes the distance between the radar and the h-th target, the relative velocity ν_h and the DoA pair (ϕ_h, θ_h), where ϕ_h and θ_h represent the azimuth angle and the elevation angle, respectively. We have $-\pi \leq \phi_h < \pi$, $0 \leq \theta_h < \pi/2$. The OFDM waveform has a FFT size of N_{fft}. The radar estimation is performed with a sequence of N_{t} OFDM symbols each with N_{f} subcarriers, since we assume that the channel parameters do not change over the N_{t} OFDM symbols. Let $f_{n_{\text{f}}}$ denote the frequency on the n_{f}-th subcarrier ($n_{\text{f}} \in \{0, \cdots, N_{\text{f}}-1\}$), which is defined as $f_{n_{\text{f}}} = f_0 + n_{\text{f}} \cdot \Delta_{\text{f}}$, where f_0 is the carrier frequency at the lower end of the band and Δ_{f} is the subcarrier spacing. Note that in a narrowband system we have $f_{n_{\text{f}}} \approx f_0$. Then the received uniformly sampled discrete-time signal at the $(m_{\text{x}}, m_{\text{y}})$-th (where $m_{\text{x}} \in \{0 \cdots M_{\text{x}}-1\}$, and $m_{\text{y}} \in \{0 \cdots M_{\text{y}}-1\}$) antenna on the n_{f}-th subcarrier in the n_{t}-th OFDM symbol is written as

$$y_{m_{\text{x}},m_{\text{y}},n_{\text{f}}}[n_{\text{t}}] = \sum_{h=0}^{H-1} k_h e^{j\beta_h} \cdot e^{-j2\pi\tau_h n_{\text{f}} \Delta_{\text{f}}} \cdot e^{\frac{j2\pi n_{\text{t}} \nu_h T_0 f_{n_{\text{f}}}}{c}} e^{j2\pi m_{\text{x}} \frac{f_{n_{\text{f}}} \Delta_{\text{x}}}{c} u_h} e^{j2\pi m_{\text{y}} \frac{f_{n_{\text{f}}} \Delta_{\text{y}}}{c} v_h} \cdot s_{n_{\text{f}}}[n_{\text{t}}] + z_{m_{\text{x}},m_{\text{y}},n_{\text{f}}}[n_{\text{t}}] \quad (1)$$

where $k_h = \sqrt{\frac{c^2 \sigma_{\text{RCS},h}}{(4\pi)^3 d_h^4 f_c^2}}$ is the unknown attenuation coefficient defined as in [2], $\sigma_{\text{RCS},h}$ denotes the radar cross-section factor, c is the speed of the light. The OFDM symbol duration is given by $T_0 = \frac{1}{\Delta_{\text{f}}} + T_G$, where T_G is the guard interval. The random phase shift is denoted as β_h. The transmitted symbol is $s_{n_{\text{f}}}[n_{\text{t}}] \in \mathbb{C}$ and the transmit power is restricted such that $\mathrm{E}\{\sum_{n_{\text{f}}=1}^{N_{\text{fft}}} |s_{n_{\text{f}}}[n_{\text{t}}]|^2\} = P_{\text{T}}, \forall n_{\text{t}}$. The term $z_{m_{\text{x}},m_{\text{y}},n_{\text{f}}}[n_{\text{t}}]$ denotes the zero-mean circularly symmetric complex Gaussian (ZMCSCG) noise with variance $\mathbb{E}\{|z_{m_{\text{x}},m_{\text{y}},n_{\text{f}}}[n_{\text{t}}]|^2\} = \sigma_{\text{n}}^2$, $\forall m_{\text{x}}, m_{\text{y}}, n_{\text{f}}, n_{\text{t}}$. Furthermore, we define the direction cosines $u_h = \cos(\phi_h)\cos(\theta_h)$ and $v_h = \sin(\phi_h)\cos(\theta_h)$, and the antenna spacings are denoted as Δ_{x} and Δ_{y}.

The communication signal $s_{n_{\text{f}}}[n_{\text{t}}]$ is is assumed to be random, but obviously it is known at the co-located radar receiver. Therefore, it can be removed from equation (1) by division and we obtain

$$r_{m_{\text{x}},m_{\text{y}},n_{\text{f}}}[n_{\text{t}}] = y_{m_{\text{x}},m_{\text{y}},n_{\text{f}}}[n_{\text{t}}] / s_{n_{\text{f}}}[n_{\text{t}}]. \quad (2)$$

Given $r_{m_{\text{x}},m_{\text{y}},n_{\text{f}}}[n_{\text{t}}]$, our goal is to estimate the parameters τ_h, ν_h, ϕ_h, and θ_h. Although the estimation can be provided simply by using just one subcarrier, it does not fully exploit the frequency diversity of the OFDM waveform. Moreover, it will limit the distance resolution of the radar, which depends on the bandwidth of the effective waveform. It is our goal to develop coherent parameter estimation methods which use all the subcarriers.

III. INTERPOLATION BASED COHERENT PARAMETER ESTIMATION

Our proposed interpolation based coherent parameter estimation algorithm consists of two steps. In the first step, the received signals on different subcarriers are preprocessed by using an interpolation algorithm such that an equivalent narrowband OFDM system is obtained, i.e., the effective subcarrier frequency $\tilde{f}_{n_{\text{f}}} = f_0$, $\forall n_{\text{f}}$. In the second step, multidimensional parameter estimation schemes such as the low complexity R-D periodogram and the high resolution R-D Unitary Tensor-ESPRIT algorithm are applied to the equivalent narrowband OFDM signal.

III-A. Pre-processing via Interpolation

The target of the pre-processing step is to obtain an equivalent narrowband model of (2), i.e.,

$$\tilde{r}_{m_{\text{x}},m_{\text{y}},n_{\text{f}}}[n_{\text{t}}] = \sum_{h=0}^{H-1} k_h e^{j\beta_h} e^{-j2\pi\tau_h n_{\text{f}} \Delta_{\text{f}}} \cdot e^{\frac{j2\pi n_{\text{t}} \nu_h T_{\text{s}} f_0}{c}} \cdot e^{j2\pi m_{\text{x}} \frac{f_0 \Delta_{\text{x}}}{c} u_h} e^{j2\pi m_{\text{y}} \frac{f_0 \Delta_{\text{y}}}{c} v_h} + \tilde{z}_{m_{\text{x}},m_{\text{y}},n_{\text{f}}}[n_{\text{t}}], \quad (3)$$

where $\tilde{z}_{m_{\text{x}},m_{\text{y}},n_{\text{f}}}[n_{\text{t}}]$ is ZMCSCG noise. Let $\tilde{r}_{m_{\text{x}},m_{\text{y}},n_{\text{f}}}[n_{\text{t}}]$ denote the $(m_{\text{x}}, m_{\text{y}}, n_{\text{f}}, n_{\text{t}})$-th element of a four-dimensional tensor. Then the tensor representation of the equivalent system model is given by

$$\boldsymbol{\mathcal{R}} = \sum_{h=0}^{H-1} \tilde{k}_h \circ \boldsymbol{a}_h \circ \boldsymbol{b}_h \circ \boldsymbol{c}_h \circ \boldsymbol{d}_h + \boldsymbol{\mathcal{Z}} \in \mathbb{C}^{M_{\text{x}} \times M_{\text{y}} \times N_{\text{f}} \times N_{\text{t}}}, \quad (4)$$

where $\tilde{k}_h = k_h e^{j\beta_h}$ and we have

$$\boldsymbol{a}_h = \begin{bmatrix} 1 & e^{j2\pi \frac{f_0 \Delta_{\text{x}}}{c} u_h} & \cdots & e^{j2\pi (M_{\text{x}}-1) \frac{f_0 \Delta_{\text{x}}}{c} u_h} \end{bmatrix} \in \mathbb{C}^{M_{\text{x}}}$$
$$\boldsymbol{b}_h = \begin{bmatrix} 1 & e^{j2\pi \frac{f_0 \Delta_{\text{y}}}{c} v_h} & \cdots & e^{j2\pi (M_{\text{y}}-1) \frac{f_0 \Delta_{\text{y}}}{c} v_h} \end{bmatrix} \in \mathbb{C}^{M_{\text{y}}}$$
$$\boldsymbol{c}_h = \begin{bmatrix} 1 & e^{-j2\pi\tau_h \Delta_{\text{f}}} & \cdots & e^{-j2\pi\tau_h (N_{\text{f}}-1)\Delta_{\text{f}}} \end{bmatrix} \in \mathbb{C}^{N_{\text{f}}}$$
$$\boldsymbol{d}_h = \begin{bmatrix} 1 & e^{\frac{j2\pi \nu_h T_{\text{s}} f_0}{c}} & \cdots & e^{\frac{j2\pi (N_{\text{t}}-1) \nu_h T_{\text{s}} f_0}{c}} \end{bmatrix} \in \mathbb{C}^{N_{\text{t}}}$$

Theoretically, this narrowband equivalent model can be obtained by reconstructing a continuous signal, followed by sampling with a decreased sampling interval. Taking the exponential term of the relative velocity in $\boldsymbol{d}_h$ as an example, this implies that using a single antenna the n_{t}-th OFDM symbol at the n_{f}-th subcarrier is obtained at the time instant

$$t_{n_{\text{f}},n_{\text{t}}} = \frac{n_{\text{t}} f_0 T_{\text{s}}}{f_{n_{\text{f}}}}, \quad (5)$$

instead of $n_{\text{t}} T_{\text{s}}$ for $n_{\text{t}} \in \{0, \cdots N_{\text{t}}-1\}$. Similarly in the spatial domains new samples (in $\boldsymbol{a}_h$ and $\boldsymbol{b}_h$) are taken at the position

$$d_{n_{\text{f}},m_{\text{x}}} = \frac{m_{\text{x}} f_0 \Delta_{\text{x}}}{f_{n_{\text{f}}}} \quad \text{and} \quad d_{n_{\text{f}},m_{\text{y}}} = \frac{m_{\text{y}} f_0 \Delta_{\text{y}}}{f_{n_{\text{f}}}}. \quad (6)$$

Under ideal conditions a perfect resampling is provided by the Shannon-Whittaker interpolation [13], which is also used in [10]. However, practically the Shannon-Whittaker interpolation cannot provide perfect reconstruction for a time-limited signal and it has a high computational complexity. Therefore, this motivates us to study alternative interpolation methods, which can be used to obtain (3) approximately but they have a much lower computational complexity.

More precisely, in this paper we apply the linear interpolation method and the cubic spline interpolation method [14]. The former one has a constant computational complexity but yields slightly larger interpolation errors. The latter one has a cubic complexity but produces a smoother fitting curve. If the linear interpolation is used, then $\tilde{r}_{m_{\text{x}},m_{\text{y}},n_{\text{f}}}[n_{\text{t}}]$ is computed by

$$\tilde{r}_{m_{\text{x}},m_{\text{y}},n_{\text{f}}}[n_{\text{t}}] = r_{m_{\text{x}},m_{\text{y}},n_{\text{f}}}[n_{\text{t}}] + \frac{t_{n_{\text{f}},n_{\text{t}}} (r_{m_{\text{x}},m_{\text{y}},n_{\text{f}}}[n_{\text{t}}+1] - r_{m_{\text{x}},m_{\text{y}},n_{\text{f}}}[n_{\text{t}}])}{T_{\text{s}}}. \quad (7)$$

This linear interpolation should also be applied on the two spatial domains. We perform a multi-dimensional interpolation by sequentially applying the one-dimensional interpolation.

III-B. R-D Periodogram

After obtaining the equivalent narrowband signal model in (3) we can apply the parameter estimation method to estimate τ_h, ν_h, ϕ_h, and θ_h. The first algorithm we introduce is the R-D periodogram as an extension of the one described in [2]. A one-dimensional periodogram is the easiest way for spectral estimation, i.e., for a given sequence of N discrete samples $a(k)$ we compute [15]

$$S(f) = \frac{1}{N}\left|\sum_{k=0}^{N-1} a(k)e^{j2\pi fk}\right|^2.$$

Then the spectral components are obtained by searching the peaks in $S(f)$. Furthermore, a digital domain periodogram is realized using a T-length FFT of the discrete samples. Therefore the resolution is inversely proportional to T. In our case a four-dimensional periodogram is required. To this end we perform the FFTs over four dimensions sequentially. Let $\tilde{\boldsymbol{\mathcal{R}}} \in \mathbb{C}^{p_1\times p_2\times p_3\times p_4}$ denote a tensor, whose r-th dimension ($r \in \{1,2,3,4\}$) is obtained by truncating the slices along the r-th dimension of $\boldsymbol{\mathcal{R}}$ if p_r is smaller than the length of the r-th dimension of $\boldsymbol{\mathcal{R}}$, or by padding zero slices along the r-th dimension of $\boldsymbol{\mathcal{R}}$ if p_r is not less than the length of the r-th dimension of $\boldsymbol{\mathcal{R}}$. Then by using the tensor notation in (4) we first compute

$$\boldsymbol{\mathcal{P}} = \tilde{\boldsymbol{\mathcal{R}}} \times_1 \boldsymbol{D}_{p_1} \times_2 \boldsymbol{D}_{p_2} \times_3 \boldsymbol{D}_{p_3}^{\mathrm{H}} \times_4 \boldsymbol{D}_{p_4}, \tag{8}$$

where $\boldsymbol{D}_{p_r}$ is the $p_r \times p_r$ DFT matrix. Then the R-D periodogram is obtained as

$$S(i_1,i_2,i_3,i_4) = \frac{1}{M_{\mathrm{x}}M_{\mathrm{y}}N_{\mathrm{f}}N_{\mathrm{t}}}|\boldsymbol{\mathcal{P}}_{i_1,i_2,i_3,i_4}|^2, \tag{9}$$

where $\boldsymbol{\mathcal{P}}_{i_1,i_2,i_3,i_4}$ is the (i_1,i_2,i_3,i_4)-th element of $\boldsymbol{\mathcal{P}}$ and we have $i_1 \in \{1,\cdots,p_1\}$, $i_2 \in \{1,\cdots,p_2\}$, $i_3 \in \{1,\cdots,p_3\}$, and $i_4 \in \{1,\cdots,p_4\}$. Finally, the computational complexity of the R-D periodogram is dominated by equation (8), which is given by $\mathcal{O}(p_1p_2p_3p_4(p_1+p_2+p_3+p_4))$. Note that the adaptive implementation of (8) introduced in Section 3.3.2 of [2] can further reduce the overall computational complexity.

III-C. R-D Wideband Unitary Tensor-ESPRIT

In this section we introduce a closed-form high-resolution parameter estimation method, which is based on the R-D Unitary Tensor-ESPRIT algorithm in [11]. The R-D Unitary Tensor-ESPRIT algorithm is a real-valued Tensor-ESPRIT algorithm, which has a lower computationally complexity compared to Tensor-ESPRIT algorithms that are based on a complex-valued tensor decomposition [11]. Next, we briefly describe how to extend the R-D Unitary Tensor-ESPRIT algorithm to our problem.

First, define $\bar{f}_1 = -2\tau_h n_{\mathrm{f}}\Delta_{\mathrm{f}}$ and $\bar{f}_2 = \frac{2\nu_h T_{\mathrm{s}} f_0}{c}$. Assume that $\bar{f}_1 \in (-2,0]$ and $\bar{f}_2 \in (-1,1]$. Then we can interpret the exponential terms as a function of time delays and relative velocities as virtual uniform linear arrays (ULAs) with spatial frequencies $\bar{f}_1$ and $\bar{f}_2$, respectively. The tensor-based spatial smoothing (TB-SS) technique can be used to extend the number of available snapshots and to decorrelate coherent targets. Let us define $L = L_1L_2L_3L_4$ and $M_r = Z - L_r + 1$, where $Z \in \{M_{\mathrm{x}}, M_{\mathrm{y}}, N_{\mathrm{f}}, N_{\mathrm{t}}\}$. Then the R-D spatial smoothing is performed over $\boldsymbol{\mathcal{R}}$ by following exactly Section IV of [16] and we obtain a new $\boldsymbol{\mathcal{R}}_{\mathrm{ss}} \in \mathbb{C}^{M_1\times M_2\times M_3\times M_4\times L}$.

Next, we define the forward-backward averaged version of the tensor $\boldsymbol{\mathcal{R}}_{\mathrm{ss}}$ as

$$\boldsymbol{\mathcal{F}} = \left[\boldsymbol{\mathcal{R}}_{\mathrm{ss}} \llcorner_5 \boldsymbol{\mathcal{R}}_{\mathrm{ss}} \times_1 \boldsymbol{\Pi}_{M_1} \times_2 \boldsymbol{\Pi}_{M_2} \times_3 \boldsymbol{\Pi}_{M_3} \times_4 \boldsymbol{\Pi}_{M_4} \times_5 \boldsymbol{\Pi}_L\right].$$

Then the tensor $\boldsymbol{\mathcal{F}} \in \mathbb{C}^{M_1\times M_2\times M_3\times M_4\times L}$ is a centro-Hermitian Tensor. The proof is straightforward according to Lemma 3 in [11].

Algorithm 1 R-D Wideband Coherent Parameter Estimation Framework

1: **Input:** $y_{m_{\mathrm{x}},m_{\mathrm{y}},n_{\mathrm{f}}}[n_{\mathrm{t}}]$, $s_{n_{\mathrm{f}}}[n_{\mathrm{t}}]$, $\forall m_{\mathrm{x}}, m_{\mathrm{y}}, n_{\mathrm{f}}, n_{\mathrm{t}}$. If the R-D periodogram is used, set p_1, p_2, p_3, and p_4. If R-D Unitary Tensor-ESPRIT is used, set L_1, L_2, L_3, and L_4.
2: **Main step:**
3: Obtain $\boldsymbol{\mathcal{R}}$ by using the linear interpolation method in (7) or the spline interpolation method.
4: **if** R-D periodogram **then**
5: Compute (8) and (9).
6: **else if** R-D Wideband Unitary Tensor-ESPRIT **then**
7: Obtain $\boldsymbol{\mathcal{R}}_{\mathrm{ss}}$ using TB-SS in [16]
8: Estimate the tensor rank of H using R-D EFT in [17]
9: Estimate the tensor-based signal subspace $\hat{\boldsymbol{\mathcal{U}}}_{\mathrm{s}}$ using (**??**)
10: Compute the LS solution of the shift invariance equation as in [11]
11: Compute the SSD to obtain automatically paired spatial frequencies u_h, v_h, $\bar{f}_1$, and $\bar{f}_2$ as in [11]
12: **end if**
13: **Output:** τ_h, ν_h, ϕ_h, and θ_h, $\forall h$.

Therefore we can map the centro-Hermitian tensor $\boldsymbol{\mathcal{F}}$ into a real-valued tensor $\boldsymbol{\mathcal{F}}_{\mathrm{r}}$ by computing [11]

$$\boldsymbol{\mathcal{F}}_{\mathrm{r}} = \boldsymbol{\mathcal{F}} \times_1 \boldsymbol{Q}_{M_1} \times_2 \boldsymbol{Q}_{M_2} \times_3 \boldsymbol{Q}_{M_3} \times_4 \boldsymbol{Q}_{M_4} \times_5 \boldsymbol{Q}_{2L}, \tag{10}$$

where matrix $\boldsymbol{Q}_m$ is assumed to be left-$\boldsymbol{\Pi}$-real. Next, we estimate the model order H of the real-valued tensor $\boldsymbol{\mathcal{F}}_{\mathrm{r}}$ by using the R-D exponential fitting test (R-D EFT) in [17]. According to [11], the rest of the R-D Wideband Unitary Tensor-ESPRIT algorithm consists of three steps, i.e., estimating the real-valued signal subspace, solving the linear R-D shift invariance equations using least squares (LS), and computing the simultaneous Schur decomposition (SSD) to obtain automatically paired frequencies u_h, v_h, $\bar{f}_1$, and $\bar{f}_2$. Except for the tensor-based signal subspace estimation step, the implementation of R-D Wideband Unitary Tensor-ESPRIT is exactly the same as in [11]. To avoid the computation of the truncated core tensor of the HOSVD of the tensor $\boldsymbol{\mathcal{F}}_r$, we use the following relationship between the SVD-based and the HOSVD-based subspace estimates [18], [19],

$$\left[\hat{\boldsymbol{\mathcal{U}}}_{\mathrm{s}}\right]_{(5)}^{\mathrm{T}} = \left((\hat{\boldsymbol{U}}_{\mathrm{s},1}\hat{\boldsymbol{U}}_{\mathrm{s},1}^{\mathrm{H}}) \otimes (\hat{\boldsymbol{U}}_{\mathrm{s},2}\hat{\boldsymbol{U}}_{\mathrm{s},2}^{\mathrm{H}}) \otimes (\hat{\boldsymbol{U}}_{\mathrm{s},3}\hat{\boldsymbol{U}}_{\mathrm{s},3}^{\mathrm{H}}) \otimes (\hat{\boldsymbol{U}}_{\mathrm{s},4}\hat{\boldsymbol{U}}_{\mathrm{s},4}^{\mathrm{H}})\right) \cdot \hat{\boldsymbol{U}}_{\mathrm{s}},$$

where $\hat{\boldsymbol{\mathcal{U}}}_{\mathrm{s}} \in \mathbb{R}^{M_1\times M_2\times M_3\times M_4\times H}$ and $\hat{\boldsymbol{U}}_{\mathrm{s}} \in \mathbb{R}^{M_1M_2M_3M_4\times H}$ represent the tensor-based and matrix-based signal subspace estimate, respectively. The matrices $\hat{\boldsymbol{U}}_{\mathrm{s},r} \in \mathbb{R}^{M_r\times H}$ and $\hat{\boldsymbol{U}}_{\mathrm{s}}$ consist of the first H left singular vectors of the r-mode unfolding $[\boldsymbol{\mathcal{F}}_{\mathrm{r}}]_{(r)}$ ($r \in \{1,2,3,4\}$) and $[\boldsymbol{\mathcal{F}}_{\mathrm{r}}]_{(5)}^{\mathrm{T}}$, respectively. Therefore, these matrices can be obtained by computing the truncated SVDs of the corresponding unfoldings, each of which yield a computational complexity of order $\mathcal{O}(M_1M_2M_3M_4LH)$. Finally, the computational complexity of our proposed R-D Wideband Unitary Tensor-ESPRIT is dominated by computing equation (**??**), which has the order of $\mathcal{O}(M_1^2M_2^2M_3^2M_4^2H)$.

To summarize, the proposed interpolation based coherent parameter estimation framework is described in Algorithm 1.

Remark 1. *The interpolation errors increase when the subcarrier index and the antenna index are large. To reduce the errors one could consider to use oversampling such that those frequencies are kept low for any possible values of the parameters of interest (relative velocity and DoAs). Windowing can also decrease interpolation errors especially for the Shannon-Whittaker interpolation. But it cannot be used when ESPRIT-type algorithms are applied, because it will destroy the shift invariant structure of the measurements.*

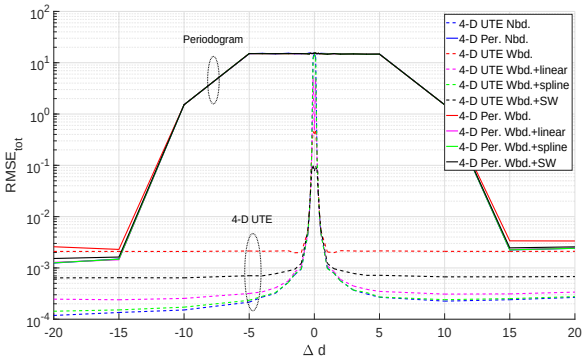

Fig. 1. Comparison of the achieved resolution for the proposed algorithms in terms of $\mathrm{RMSE}_{\mathrm{tot}}$.

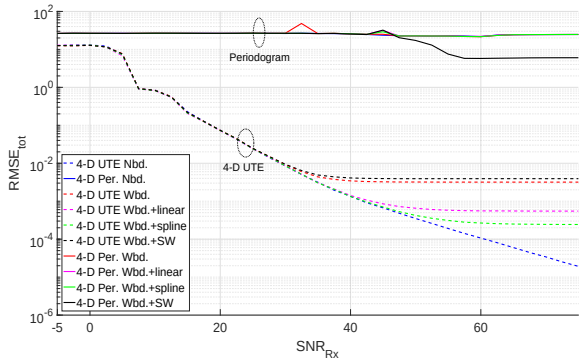

Fig. 2. Comparison of the $\mathrm{RMSE}_{\mathrm{tot}}$ as a function of the received $\mathrm{SNR}_{\mathrm{Rx}}$ for target at distance $d_1 = 95$ m.

IV. SIMULATION RESULTS

In this section the proposed interpolation based coherent parameter estimation framework is evaluated using Monte Carlo simulations. During our simulations, the following assumptions are made: 1) the radar targets are considered as point scatterers; 2) we use a free space pathloss model; 3) there is no clutter in the system. Moreover, the carrier frequency is $f_0 = 24$ GHz. The OFDM symbol duration is $T_0 = 1.6$ μs. The FFT size is $N_{\mathrm{fft}} = 64$ and we set $N_{\mathrm{f}} = N_{\mathrm{fft}}$. The system bandwidth is $B = 76.8$ MHz and the subcarrier spacing is $\Delta_{\mathrm{f}} = 1.2$ MHz. The physical antenna spacing is chosen as $\Delta_{\mathrm{x}} = \Delta_{\mathrm{y}} = \frac{c}{4f_0}$, which results in oversampling in the spatial domains. Each training period consists of $N_{\mathrm{t}} = 10$ OFDM symbols. The URA is of size $M_{\mathrm{x}} \times M_{\mathrm{y}} = 5 \times 5$. The transmit power is equal to $P_{\mathrm{t}} = 40$ dBm. The noise power spectral density is $N_0 = -199$ dBm/Hz. When the R-D periodogram is used, we set $p_1 = 4M_{\mathrm{x}}$, $p_2 = 4M_{\mathrm{y}}$, $p_3 = 4N_{\mathrm{f}}$, and $p_4 = 4N_{\mathrm{t}}$. When R-D Wideband Unitary Tensor-ESPRIT is used, we set $L_1 = L_2 = 1$, $L_3 = 55$ and $L_4 = 3$. The simulation results are averaged over 1000 realizations.

The evaluation criterion is the total root mean square estimation error ($\mathrm{RMSE}_{\mathrm{tot}}$). The $\mathrm{RMSE}_{\mathrm{tot}}$ is defined as

$$\mathrm{RMSE}_{\mathrm{tot}} = \sqrt{\sum_{r=1}^{4} w_{(r)}^2 \frac{1}{H} \mathbb{E}\left\{ \sum_{h=0}^{H-1} (x_h^{(r)} - \hat{x}_h^{(r)})^2 \right\}}.$$

where $x_h^{(r)} \in \{d_h, \nu_h, u_h, v_h\}$ and $\hat{x}_h^{(r)}$ is an estimate of $x_h^{(r)}$, and $w_{(r)} = [0.5\ 1/\mathrm{m}, 2.6 \cdot 10^{-3}\ \mathrm{s/m}, 1.25, 1.25]$ a some weighting coefficients defined empirically.

In the first simulation there are two targets, i.e., $H = 2$, and our goal is to study the spatial resolution provided by the proposed algorithms. We set $\phi_1 = \phi_2 = \theta_1 = \theta_2 = 45°$, and velocities $\nu_{x,1} = \nu_{x,2} = 20$ m/s, $\nu_{y,1} = \nu_{y,2} = \nu_{z,1} = \nu_{z,2} = 0$ m/s, where $\nu_{x,h}$, $\nu_{y,h}$ and $\nu_{z,h}$ are projections of the absolute speed on Euclidean coordinates. The distance between the radar and the second target is $d = 50$ m while the distance between the radar and the first target varies from 30 m to 70 m during the simulation. Let Δd denotes the distance between the two targets. Let "Nbd" and "Wbd" denote the narrowband model in (3) and the wideband model in (1), respectively. Let "Per." and "UTE" denote the R-D periodogram and the R-D Unitary Tensor-ESPRIT algorithm, respectively. Let "linear", "spline", and "SW" represent the linear interpolation, the spline interpolation, and the Shannon-Whittaker interpolation method, respectively.

Then it can be seen in Fig. 1 that the proposed R-D Wideband Unitary Tensor-ESPRIT using any interpolation algorithm provides a significant performance gain as compared to narrowband algorithm. Notice that interpolation techniques do not improve the performance of the R-D periodogram.

In the second simulation we consider five fixed targets, i.e., $H = 5$, and the estimation error is plotted as a function of the received $\mathrm{SNR}_{\mathrm{Rx}}$ of the first target at distance $d_1 = 95$ m, which is altered via changing the noise figure NF. The parameters of five targets are chosen to be close to each other: $d_h \in \{95, 100, 105, 110, 115\}$ m, $\phi_h \in \{26°, 30°, 34°, 38°, 42°\}$, $\theta_h \in \{52°, 55°, 58°, 61°, 64°\}$ with $\nu_{x,h} = 20$ m/s and $\nu_{y,h} = \nu_{z,h} = 0$ m/s for all $h \in \{1, \cdots, 5\}$.

Fig. 2 depicts the results of second simulation. The proposed R-D Wideband Unitary Tensor-ESPRIT combined with spline interpolation provides the best performance in the wideband case. Periodogram based solutions fail to resolve such closely spaced targets. Since there are always residual interpolation errors, error floors exist for all algorithms in case of the wideband model (1) when the received $\mathrm{SNR}_{\mathrm{Rx}}$ is large. It can be observed that the gain through interpolation for UTE appears only when received $\mathrm{SNR}_{\mathrm{Rx}}$ exceeds 30 dB, which is expected since the additive noise simply overshadows differences between narrowband and wideband data models.

V. CONCLUSION

In this paper we have studied a wideband SIMO communication radar based on OFDM waveforms. The wideband assumption results in incoherent signals on different subcarriers. To reduce the incoherence we have proposed an interpolation based coherent parameter estimation framework. First, the wideband system model is converted into an approximately equivalent narrowband model by using different interpolation methods. Linear interpolation is chosen due to its lowest computational complexity, while cubic spline interpolation is used due to its low interpolation error. Then the multidimensional parameter estimation algorithms, i.e., a baseline algorithm based on the R-D periodogram and the proposed R-D Wideband Unitary Tensor-ESPRIT, are applied to provide accurate estimates. The simulation results show that the proposed algorithms outperform the Shannon-Whittaker interpolation based coherent solution as well as the direct application of the narrowband parameter estimation methods on the wideband model. Moreover, the R-D Wideband Unitary Tensor-ESPRIT algorithm provides a better resolution than the R-D periodogram. It should be noted that the application of interpolation techniques is only beneficial in the high SNR regime or in case of high fractional bandwidths.

ACKNOWLEDGMENTS

The authors acknowledge the financial support by the Carl-Zeiss-Foundation (http://carl-zeiss-stiftung.de/).

VI. REFERENCES

[1] C. Sturm and W. Wiesbeck, "Waveform design and signal processing aspects for fusion of wireless communications and

radar sensing," *Proceedings of the IEEE*, vol. 99, pp. 1236–1259, July 2011.

[2] M. Braun, *OFDM radar algorithms in mobile communication networks*, Ph.D. thesis, Karlsruhe University of Technology, 2014.

[3] C. Sturm, T. Zwick, and W. Wiesbeck, "An OFDM system concept for joint radar and communications operations," in *Proc. IEEE International Vehicular Technology Conference (VTC 2009)*, Apr. 2009.

[4] C. Sturm, M. Braun, T. Zwick, and W. Wiesbeck, "A multiple target Doppler estimation algorithm for OFDM based intelligent radar systems," in *Proc. European Radar Conference (EuRAD)*, Sept. 2010.

[5] A. D. Harper, J. T. Reed, J. L. Odom, and A. D. Lanterman, "Performance of a joint radar-communication system in doubly-selective channels," in *Proc. Systems and Computers 2015 49th Asilomar Conf. Signals*, Nov. 2015, pp. 1369–1373.

[6] J. R. Krier, M. C. Norko, J. T. Reed, R. J. Baxley, A. D. Lanterman, Xiaoli Ma, and J. R. Barry, "Performance bounds for an OFDM-based joint radar and communications system," in *Proc. MILCOM 2015 - 2015 IEEE Military Communications Conf*, Oct. 2015, pp. 511–516.

[7] P. Papadimitratos, A. D. La Fortelle, K. Evenssen, R. Brignolo, and S. Cosenza, "Vehicular communication systems: Enabling technologies, applications, and future outlook on intelligent transportation," *IEEE Communications Magazine*, vol. 47, pp. 84–95, Nov. 2009.

[8] E. Strom, H. Hartenstein, P. Santi, and W. Wiesbeck, "Vehicular communications: Ubiquitous networks for sustainable mobility," *Proceedings of the IEEE*, vol. 98, pp. 1111–1112, July 2010.

[9] P. Kumari, N. G. Prelcic, and R. W. Heath, Jr., "Investigating the IEEE 802.11ad standard for millimeter wave automotive radar," in *Proc. IEEE International Vehicular Technology Conference (VTC 2015)*, Apr. 2015.

[10] F. Raimondi, P. Comon, and O. Michel, "Wideband multilinear array processing through tensor decomposition," in *Proc. IEEE Int. Conf. on Acoustics, Speech, and Signal Processing (ICASSP)*, Shanghai, China, Mar. 2016.

[11] M. Haardt, F. Roemer, and G. Del Galdo, "Higher-order SVD based subspace estimation to improve the parameter estimation accuracy in multi-dimensional harmonic retrieval problems," *IEEE Transactions on Signal Processing*, vol. 56, pp. 3198–3213, July 2008.

[12] L. de Lathauwer, B. de Moor, and J. Vanderwalle, "A multilinear singular value decomposition," *SIAM J. Matrix Anal. Appl.*, vol. 21, no. 4, 2000.

[13] C. E. Shannon, "Communication in the presence of noise," *Proceedings of the IRE*, vol. 37, pp. 10–21, 1949.

[14] A. V. Oppenheim and R. W. Schafer, *Discrete-time signal processing*, Pearson Education Limited, 2014.

[15] S. M. Kay, *Modern Spectral Estimation*, Prentice Hall, New York, 1997.

[16] A. Thakre, M. Haardt, F. Roemer, and K. Giridhar, "Tensor-based spatial smoothing (TB-SS) using multiple snapshots," *IEEE Transactions on Signal Processing*, vol. 58, pp. 2715–2728, May 2010.

[17] J. P. C. L. da Costa, F. Roemer, M. Haardt, and R. T. de Sousa Jr, "Multi-dimensional model order selection," *EUROSIP Journal on Advances in Signal Processing*, pp. 1–13, 2011.

[18] F. Roemer, E.-K. Kasnakli, Y. Cheng, and M. Haardt, "Tensor subspace tracking via Kronecker structured projections (TeTraKron)," in *Proc. IEEE 5th Int. Workshop on Computational Advances in Multi-Sensor Adaptive Processing (CAMSAP 2013)*, Saint Martin, French Antilles, Dec. 2013.

[19] Yao Cheng, Florian Roemer, Olaa Khatib, and Martin Haardt, "Tensor subspace tracking via kronecker structured projections (tetrakron) for time-varying multidimensional harmonic retrieval," *EURASIP Journal on Advances in Signal Processing*, vol. 2014, no. 1, pp. 1–14, 2014.